scientific reports

Check for updates

OPEN

Examining the effects of biofield therapy through simultaneous assessment of electrophysiological and cellular outcomes

Lorenzo Cohen[1,5]✉, Arnaud Delorme[2,3,5], Andrew Cusimano[1], Sharmistha Chakraborty[1], Phuong Nguyen[1], Defeng Deng[1], Shafaqmuhammad Iqbal[1], Monica Nelson[1], Daoyan Wei[1], Chris Fields[4,6] & Peiying Yang[1,5]

In this case study, a self-described biofield therapy (BT) practitioner (participant) took part in multiple ($n = 60$) treatment and control (non-treatment) sessions under double-blind conditions. During the treatment phases, the participant provided BT treatment at a distance of about 12 inches from the cells, alternating with rest phases where no such efforts were made. Human pancreatic cancer cell activity was assessed using three markers – cytoskeleton changes (tubulin and β-actin) and Ca^{2+} uptake. The study examined changes in the participant's physiological parameters including electroencephalogram (EEG) and heart rate measures during the treatment of: (1) live cells and (2) either dead cells or medium only with no cells (control group). Changes in cellular outcomes and if there was an association between the participant's physiological parameters and cellular outcomes were examined. The experimental setup was a 2×2 design, contrasting cell type (live vs. control) against session type (treatment vs. non-treatment). Parallel sham-treated control cells were examined for changes in the cell parameters over time while controlling for the presence of a person in front of the cells mimicking the distance and movements of the participant. The participant's physiological data, including 64-channel EEG and heart rate, were continuously monitored throughout these sessions. We observed significant ($p < 0.01$) spectral changes in the participant's EEG during BT treatment in all frequency bands of interest, as well as in heart rate variability (HRV) (RMSSD measure; $p < 0.01$). We also observed significant differences in beta and gamma EEG and HRV (pNN50 measure) when the participant treated live but not control cells ($p = 0.02$). However, no interaction between treatment and cell type (live vs. dead cells/medium-no cells) was observed. We observed Ca^{2+} uptake increased over time during both BT and sham treatment, but the increase was significantly less for the BT group relative to the sham-treatment controls ($p = 0.03$). When using Granger causality to assess causal directional associations between cell markers and participant's physiological parameters, EEG measurements showed significant bidirectional causal effects with cell metrics, especially β-actin and intracellular Ca^{2+} levels ($p < 0.000001$). These outcomes suggest a complex relationship between physiological responses and cellular effects during BT treatment sessions. Given the study's limitations, follow-up investigations are warranted.

Keywords Biofield Therapy (BT), Pancreatic Cancer cells, Double-blind, Electroencephalogram (EEG), Heart Rate Variability (HRV), Granger Causality

Complementary and alternative medicine interventions, once viewed as fringe science, have in some cases provided novel, efficacious therapeutic interventions that are now part of conventional medicine[1]. However, some modalities are met with skepticism due to the lack of any accepted mechanistic bases for such interventions on pathophysiological processes. One such treatment modality is biofield therapy (BT), which the National Cancer Institute classifies as "energy therapy"[2]. The practice of providing BT posits that it is possible to influence

[1]The University of Texas MD Anderson Cancer Center, Houston, TX, USA. [2]Institute of Noetic Sciences, Novato, CA, USA. [3]University of California San Diego, La Jolla, CA, USA. [4]11160 Caunes Minervois, France. [5]Lorenzo Cohen, Arnaud Delorme and Peiying Yang contributed equally to this work. [6]Chris Fields is an independent researcher. ✉email: lcohen@mdanderson.org

biological processes and health outcomes across spatial or temporal distances through non-contact interventions such as Reiki, Healing Touch, Therapeutic Touch, Qigong, and other forms of treatment[3–6]. Although the mechanisms of action are unknown, research indicates that there is widespread use of BT modalities[3], belief in its effectiveness among Americans[4], and perception that it is beneficial and provides support to patients[5].

Clinical trials that have examined the effects of BTs such as Therapeutic Touch, Healing Touch, and Reiki have shown that these treatments led to improvements in subjective outcomes such as pain and anxiety and some indication of improvements in immunologic parameters[6]. Despite this, there are conflicting findings regarding the effectiveness of BT's. For example, Rao et al.[7] conducted a systematic review of BT interventions for managing non-communicable disease-related symptoms and identified 27 studies that evaluated various BT interventions, with 13 trials showing statistically significant outcomes. Other systematic reviews of BT studies have found that most evidence was against the notion that BT is more than a placebo[8]. Astin et al.[9] found that while approximately 57% of trials showed a positive treatment effect, the methodological limitations of several studies were significant. These included inadequate power, failure to control for baseline differences between study groups, heterogeneity of patients, and lack of objective outcomes. The mean overall Jadad score, a measure of study quality, was 3.6 out of a maximum of 5, indicating that many studies did not meet high methodological standards. Other reviews[10,11] came to similar conclusions, although a more recent meta-analysis study took a more positive stance[12].

However, studies such as those by Jain et al.[13] have addressed these issues by using double-blind settings and objective outcomes to demonstrate the efficacy of BT in treating 76 breast cancer survivors, showing significant biomarker changes in BT compared to placebo. Similarly, Lutgendorf[14] also conducted a blinded trial using therapeutic touch and found differences between TT and control group not only in patient-reported outcomes but also natural killer cell function. These studies suggest a positive impact of BT on illness symptoms and more objective biological outcomes, while reducing potential bias via the absence of physical contact between the healer and the participants.

Prior research limitations can be reduced by focusing on a single type of treatment modality, avoiding human subjects as the targets, and using animals or biological tissue where the placebo effect can be avoided. Further, because intersubject variability among practitioners is high, case studies have value in analyzing phenomena with minimal or disputed effects. This approach, which we implemented here, is favored for its potential to reveal statistically significant effects that group studies might miss.

While some research has been performed to assess physiological changes within the BT practitioner as they engage in the treatment process, there has been little robust evidence of these biomarkers, most likely due to the dearth of studies, variability in treatment modalities, and small sample sizes[15]. Further, to our knowledge, no studies have examined the association between the practitioner's physiology and the target type and outcomes (e.g., cell activity). These issues underscore the complexity of BT research and the need for more rigorous methodologies.

In vitro cell and in vivo animal studies are less subject to experimental biases (e.g., patient blinding, placebo effects) and have shown some evidence that BT modifies cellular function and tumor growth. For example, Gronowicz et al.[16] found BT modulated DNA synthesis and human osteoblast mineralization in culture studies[17]. In a separate series of studies, the same laboratory found that BT inhibited metastasis and modulated immune responses in a mouse breast cancer in vivo model[18]. Our prior research found that BT reduced cell viability and downregulated pAkt in non-small cell lung cancer cells[19]. We also reported that BT slowed the growth and increased necrosis/apoptosis in mouse Lewis lung carcinoma animal models[19,20] and found that BT modulated the tumor microenvironment as well as the stemness of tumor cells[20]. More recent preliminary research[21,22] found statistically significant effects of BT on cancer cell proliferation, motility, invasiveness, cell membrane potential, and protein expression.

Despite this relevant prior research, there is no accepted scientific mechanism of action of BT. There are multiple theories of consciousness compatible with biofield therapy[23]. We anticipate that developing a rigorous theoretical framework for BT will require multiple well-designed experiments across which phenomenological commonalities can be identified. The intent of the present study was, therefore, not to test any specific mechanism(s) of BT per se, but to determine if there was a statistically significant effect in both the BT practitioner and cancer cells in vitro.

The current case study involved a BT practitioner (participant) who took part in a series of treatment sessions providing BT to live cells or dead cells/medium only (no cells) in vitro in a blinded fashion while simultaneously examining changes in cell measures and physiological changes in the participant (Fig. 1). Sets of sham-treated control cells were also examined and tracked over time. The aim was to determine any potential effects of the treatment sessions on cell activity, examine changes in the physiological state of the participant when treating live cells versus control conditions (dead cells or no cells), and investigate the association between the BT's physiological state, cell activity, and their possible mutual influences.

The previous research has shown that changes in the BT practitioner could correlate with therapeutic efficacy[4,5,15,24]. By monitoring overall central nervous system activity via EEG and parasympathetic/vagal activity via HRV, the study sought to identify any measurable physiological shifts that might relate to the participant's therapeutic intent, providing a potential pathway to understanding how non-contact therapies could exert influence. The relevance of these physiological measures is grounded in the hypothesis that mental states and physiological regulation, as reflected by EEG and HRV, might influence cellular processes.

We hypothesized that BT targeting cancer cells involves one or more specific correlations between activity in the participant's brain and/or peripheral nervous system and cancer-relevant cellular processes. We tested the following hypotheses: (1a) The participant's physiology changes during treatment in a predictable manner relative to baseline; (1b) The participant's physiology will differ based on the cell type being treated; (2) Cell markers will change significantly over time during BT versus sham-treated control cells; (3) There is an association between

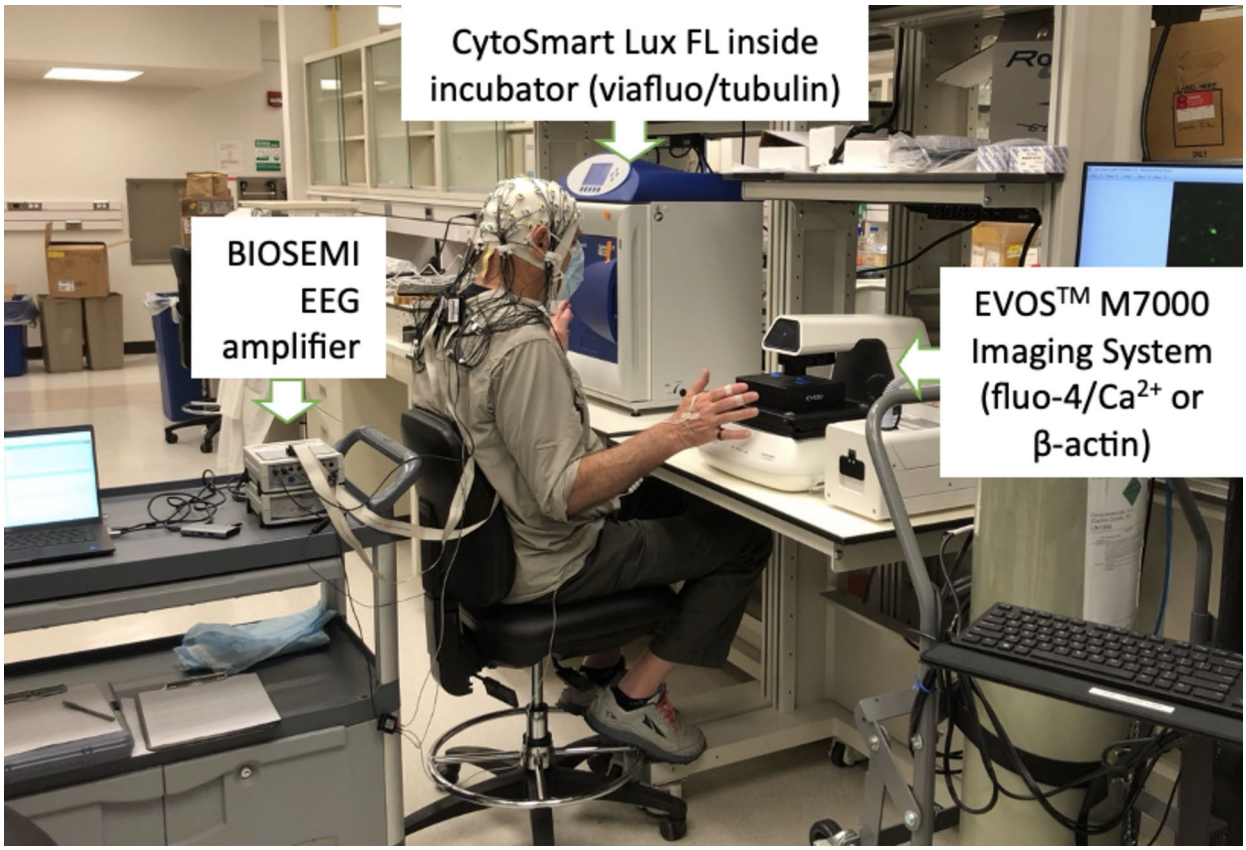

Fig. 1. Experimental setup. Participant providing non-contact biofield treatment while seated in front of pancreatic cancer cells. Cells designated for the measurement of tubulin were in the incubator equipped with the CytoSmart Lux microscope on the left. To the right of the participant, the EVOS M7000 microscope captured images of Ca^{2+} or β-actin changes. Positioned behind the participant was the EEG amplifier. Cells were enclosed and temperature regulated in the CytoSmart microscope, so the proximity of the participant was unlikely to influence outcomes, and he remained blinded to cell type. The participant's hands sometimes rested on the table and sometimes were held up. When resting on the table, the participant's hand never touched the cell measurement devices.

the participant's physiological changes and changes in cell markers. The study used analytical techniques including entanglement analysis and classical correlations (reported in Fields et al. (2024)[25]), where we did not find evidence for entanglement but did report significant correlations between the participant's physiological changes and cell marker changes. For this paper, results for hypotheses 1–3 are presented in detail, as well as conducting post-hoc exploratory Granger causality analysis to further understand directionality of the classical correlations.

Results

Changes in participant's physiology based on treatment condition and cell type

Changes in EEG spectral power were evaluated during the treatment versus the baseline condition and when the participant was treating live pancreatic cancer cells (commercially available PANC-1 cells not from the participant) versus dead cells or medium-no cells. This was conducted using a 2 × 2 factorial design (treatment vs. baseline by live cells vs. dead cells/medium-no cells) (see Fig. 2 and Methods).

EEG spectral power

Four frequency bands were analyzed: theta (4 to 8 Hz), alpha (8 to 12 Hz), beta (8 to 22 Hz), and gamma (30 to 45 Hz). There were two baseline periods (immediately before the start and after BT treatment) and two treatment periods (first 5 min and last 5 min) of the 15-minute treatment sessions (see Fig. 2). We tested for differences between the two baselines and found no significant channel difference in the frequency bands. This suggests that the participant's EEG returned to the pre-treatment baseline immediately after stopping the treatment. We also tested for any differences between the two treatment periods and found no significant differences in any frequency bands for any channels. This suggests stable EEG across the 15-minute treatment period. In the rest of this section, "treatment" refers to the two treatment periods combined, and baseline refers to the pre- and post-baseline data combined.

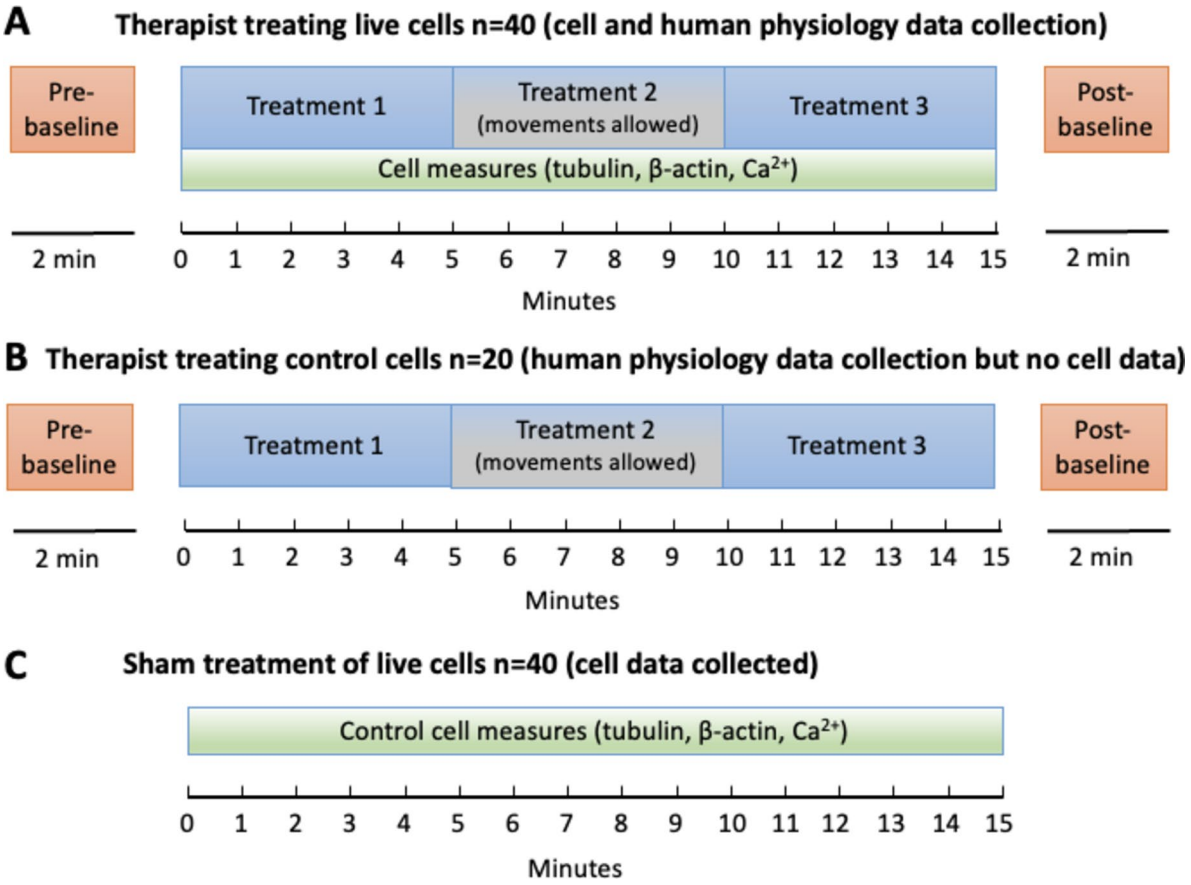

Fig. 2. Graphical representation of the study design. (**A**) Treatment condition where the BT participant was treating live cells, and cell data and human physiology were collected. (**B**) Control condition where the participant provided treatment to petri dishes with dead cells or medium-no cells and human physiology data was collected. (**C**) Cell control condition, where a sham participant was present and only cell data was collected. The participant was blind to the cell target in conditions A and B.

EEG freq. range	Baseline vs. treatment (*p*)	Cell type (live vs. dead/medium-no cells) (*p*)	Interaction (*p*)
Theta 4–8 Hz	43.76 ($p < 0.01$)	4.89 (*ns*)	0.35 (*ns*)
Alpha 8–12 Hz	37.41 ($p < 0.02$)	5.55 (*ns*)	0.68 (*ns*)
Beta 18–22 Hz	96.42 ($p < 0.01$)	25.05 ($p = 0.05$)	1.34 (*ns*)
Gamma 30–45 Hz	144.10 ($p < 0.01$)	24.99 ($p = 0.02$)	2.99 (*ns*)

Table 1. BT participant's EEG spectral power results for treatment x cell type. The first value in columns 2 and 3 are the maximum statistical value (F) across each frequency range. The value in parenthesis shows the minimum p-value across channels after correction for multiple comparisons (see Methods).

The study utilized a 2×2 factorial design, examining a comparison between treatment and baseline in the second column, cell type in the third column, and the interaction between these two factors in the final column. Results are presented in Table 1.

The comparison between treatment and baseline showed significant differences across all frequency bands, revealing variations in spectral power during treatment compared to baseline, with the largest differences in beta and gamma bands. Additionally, significant distinctions were noted in the spectral power within the beta and gamma frequency bands as a function of cell type, where live cells differed from control cells. There were no significant interaction effects, indicating that the influence of cell type on spectral power did not vary between treatment and baseline.

Another way to appreciate these results is by using EEG scalp power topographies. Figure 3 represents the results shown in Table 1. The effect of cell type is modest but remains significant even after correction for multiple comparisons. This effect was also visible in the gamma frequency band with similar topography. The interaction of scalp topography is not shown since no electrode was significant for the interaction between the two factors in any frequency bands.

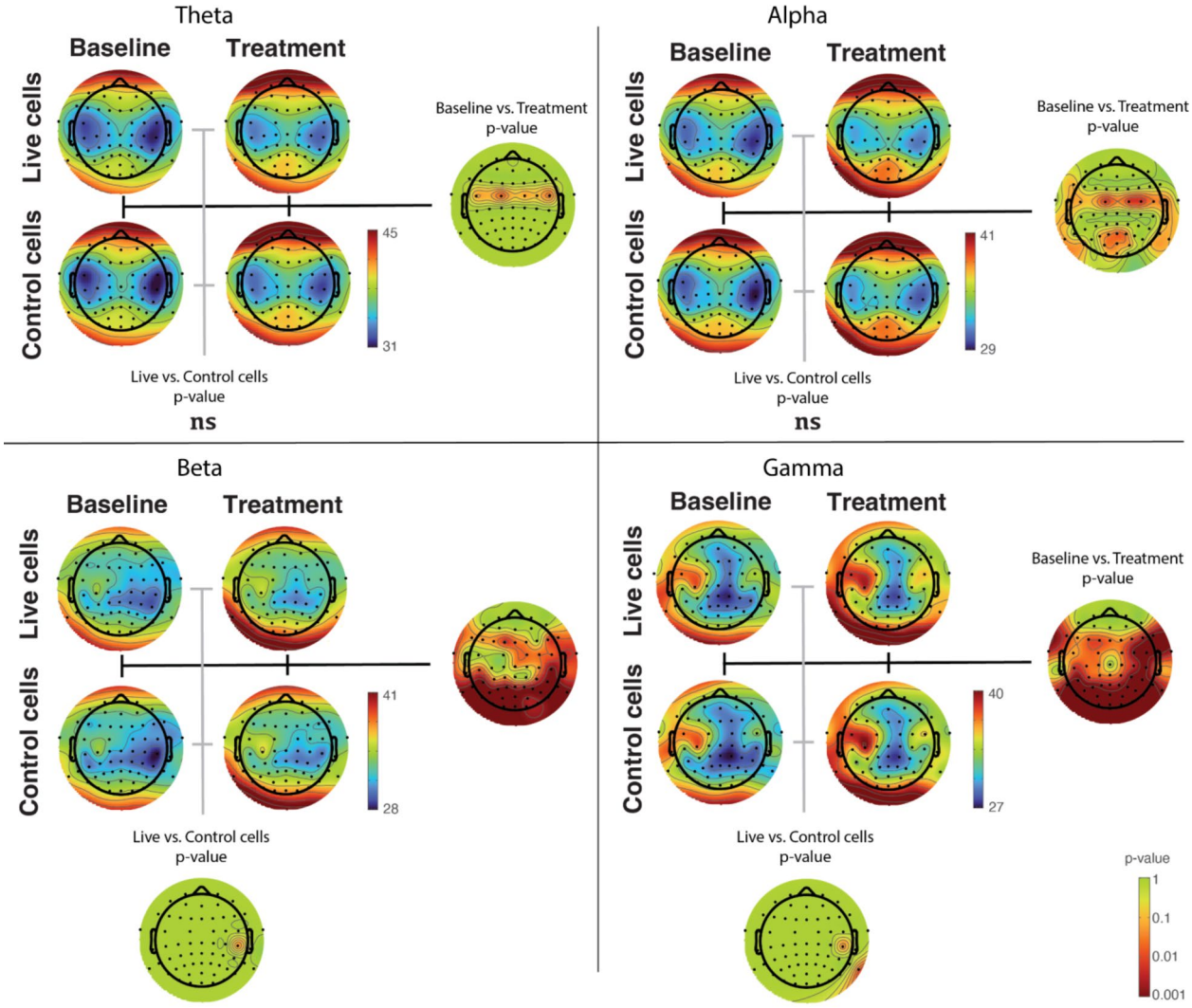

Fig. 3. Participant's EEG spectral power in all frequency bands in the 2 × 2 ANOVA design (cell type x treatment conditions). Spectral power is shown in the central region of each panel, and significance is shown on the right for the treatment effect and below for the cell type effect after correction for multiple comparisons. The significance scale (after FDR correction for multiple comparisons) is shown using a logarithmic scale.

Measure	Baseline vs. treatment (*p*)	Cell type (live vs. dead/medium-no cells) (*p*)	Interaction (*p*)
NN-mean	0.37 (*ns*)	3.14 (*ns*)	0.08 (*ns*)
NN-SD	0.21 (*ns*)	5.45 (*ns*)	0.15 (*ns*)
RMSSD	10.82 ($p = 0.02$) ⇓	0.23 (*ns*)	0.10 (*ns*)
pNN50	0.12 (*ns*)	8.27 ($p = 0.05$) ⇑	0.39 (*ns*)
HF-HRV	0.41 (*ns*)	2.53 (*ns*)	0.01 (*ns*)

Table 2. Therapist ECG and HRV results by treatment/baseline and cell type. The first value in each cell is the maximum statistical value (F) across the ECG or HRV outcomes. The value in parenthesis shows the p-value after correction for multiple comparisons. The downward arrow for RMSSD indicates a decrease in that measure for treatment compared to baseline. The upward arrow for cell type for pNN50 indicates an increase in that measure in the dead/medium condition vs. the live cell condition.

ECG and HRV results

Table 2 displays the ECG and HRV results for the treatment versus the baseline condition and live cell vs. control (2 × 2 design). We observed no significant main effects or interaction for heart rate difference between conditions (NN-mean). The RMSSD HRC measure was lower in the treatment versus baseline period, indicating a decrease in the participant's parasympathetic nervous system (PNS) activity during treatment (i.e., increased

sympathetic activation). The pNN50 HRV measure was marginally significant for the cell type main effect and reflected lower PNS activity in the participant associated with providing treatment to live pancreatic cancer cells versus dead cells/medium-no cells. There were no significant differences in cell type or treatment/baseline for NN-SD and HF-HRV and no interaction effects for any of the variables (see Methods section for the definition of these measures).

Influence of treatment on cell activity

We assessed whether cell activity was influenced by BT treatment by comparing cell marker (tubulin, Ca^{2+}, and β-actin) changes over time for the cells exposed to BT treatment versus the sham-treatment control cells that were kept in a separate room (see Methods and Fig. 2 comparing panels A and C). There were 40 recording sessions for treatment and 40 sham-treatment control sessions. Cell markers were measured at baseline and then every minute during the 15-minute treatment period. Values during each treatment session were subtracted from their respective baseline starting point, measured in the minute before treatment started, to create change from baseline over time.

Because the continuous measurement of cell markers across time introduces a correlation in time (supplementary Fig. 1), we used a mixed model with treatment as a categorical variable, regressing out the contribution of the minute variable (cell_measure ~ treatment + (minutes | treatment)). We resorted to using non-parametric statistics due to the residuals not being normally distributed (see Methods). Tubulin decreased over time and β-actin increased over time with no significant differences between BT treatment and sham treatment (tubulin: effect size estimate of 0.16 between treatment and control, $p = 0.63$; β-actin: effect size estimate = 0.41 between treatment and control, $p = 0.37$) were not significant. However, although Ca^{2+} increased over time for both groups, there was a significant group difference (effect size estimate of 0.66 between BT treatment and sham treatment, $p = 0.03$), with significantly less of an increase in Ca^{2+} over time due to BT treatment.

As a positive control to determine if the BT treatment was having an effect on the PANC-1 cells, we examined the effects of BT treatment and sham treatment on decreasing the invasiveness of the cancer cells 48 h after the treatment sessions. This was carried out during one of the 15-minute treatment sessions on two separate days during the 10-day experiment. Figure 4 shows BT significantly reduced the invasiveness potential relative to sham controls on two separate days during the conduct of the trial ($p < 0.0001$), consistent with our prior work[22].

Associations between participant EEG/HRV and cell outcomes

To better explore any causal associations between the participant and cell biomarkers, in post-hoc analyses we used Granger causality analyses[26]. We examined whether the participant's physiological data influenced the cell marker data in a causal manner and whether the cell marker data influenced the participant's physiological data in a causal manner (see Methods).

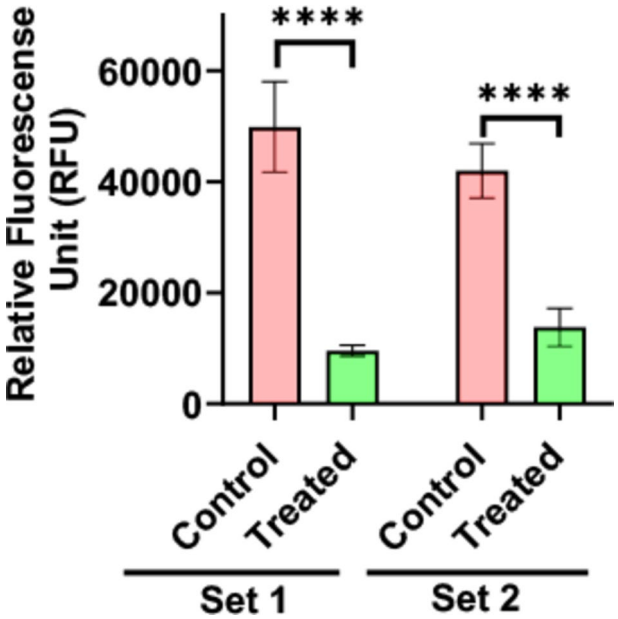

Fig. 4. Biofield therapy (BT) markedly inhibited the invasiveness of PANC-1 cells. Invasion of PANC-1 cells was measured 48 h after 15-minute BT treatment (Treated) or 15-minute sham control (Control) in experimental series one (Set 1) and experimental series two (Set 2). GraphPad Prism (Version 10) was used for the statistical analysis to test for group differences using t tests. Data are presented as mean ± SD. **** is $p < 0.0001$.

Causal influences between EEG spectral power and cell marker data

The cell marker data has a 1-minute time resolution. Therefore, we transformed the EEG data to obtain the same time resolution, computing spectral power over 1-minute periods (see Methods). Multivariate Granger causality relies on autoregressive models, specifying that an output variable depends linearly on its previous values and the previous values of other variables. A critical parameter – the model order – thus determines how many previous values the model should consider. We first searched for the optimal model order (see Methods), which was equal to 6. A model order of 6 indicates that the model looks at 6 min in the past. Significance was assessed by comparing the model during treatment sessions and the same model with the same EEG/HRV measures but replacing the cell marker data with the corresponding sham-treatment control cell marker data (panels A and C in Fig. 2). We were specifically interested in assessing the significance of the Granger causality terms related to the cross-influence between EEG/HRV and cell measures.

We observed a significant causal influence of tubulin on EEG. Tubulin Granger-causes EEG spectral power measurements in beta and gamma bands. However, EEG in all frequency bands did not Granger-caused tubulin (Fig. 5). Ca^{2+} did not Granger-cause any EEG spectral measurements. However, EEG in all frequency bands Granger-caused Ca^{2+} measurements. Most of the causal influence was concentrated in the occipital and temporal brain regions (see Fig. 5). β-actin did not Granger-cause any EEG measures or vice-versa.

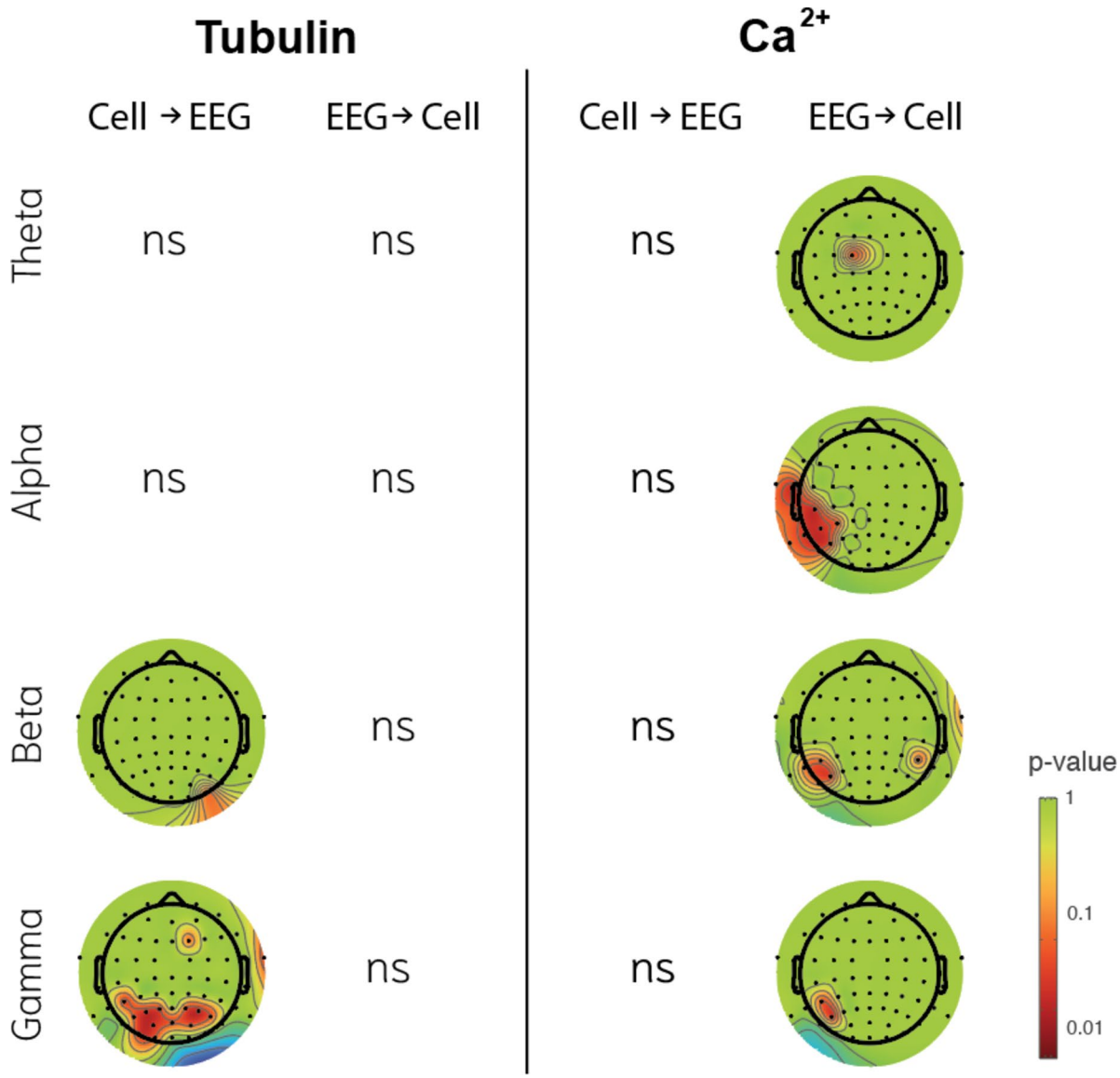

Fig. 5. Significance of Granger causality between brain EEG signals in different frequency bands (theta, alpha, beta, gamma) and cell data (tubulin and Ca^{2+}). β-actin is not represented because the values were not significant in either direction - Cell to EEG or EEG to Cell. The logarithmic scale indicates significance after FDR correction for multiple comparisons (electrodes in red are below 0.05 and significant).

Causal influences between ECG/HRV and cell marker data

We also used a model of order 6 for the ECG/HRV data and performed the same type of analysis testing to see if the cell measures Granger-caused ECG/HRV parameter outcomes and vice versa. None of the statistical values remained significant after adjusting for false discovery rate (FDR) corrections (data not shown).

Discussion

In this case study, the physiology of a BT practitioner (EEG spectral power and HRV) was measured during the treatment of two pancreatic cancer cell conditions (live cells vs. control (dead or absent)) and compared between treatment and baseline/resting sessions. In support of hypothesis 1a, we observed significant spectral changes in the participant's EEG during treatment versus baseline in all frequency bands of interest and an increase in sympathetic nervous system arousal. In support of hypothesis 1b, we also observed significant differences in beta and gamma EEG and HRV (pNN50) when the participant was treating live cells versus the control cell condition (dead cells or medium-no cells). However, no interaction between treatment and cell type was observed. In addition to the physiological data, cell activity was assessed using three markers – tubulin, β-actin, and Ca^{2+} – to determine the association between the participant's physiological states and cell activity. In support of hypothesis 2, we observed that Ca^{2+} increased over time but significantly less under the BT treatment condition versus sham treatment, suggesting a notable effect of the treatment on cellular processes. In support of hypothesis 3, our prior paper noted significant correlations between the participant's physiological states and cell activity (reported in Fields et al. (2024)[25]. In our present study, when using Granger causality to assess the potential causal associations between the participant's physiological states and cell activity, we showed significant bidirectional causality with EEG and cell metrics, especially tubulin and Ca^{2+}.

Case studies for unexpected phenomena

Case studies that analyze extensive data sets offer unique benefits compared to group studies, particularly when the magnitude of the effects being studied are small, and there is a common assumption that such effects are likely non-existent, as in this situation. Our method relies entirely on empirical evidence since the underlying processes of BT, should they exist, remain unknown. To challenge the assumption of no effect, it suffices to demonstrate its presence in just one individual engaging in BT. This strategy is particularly useful for establishing the existence of small-magnitude effects, as it reduces the inter-individual noise and variability inherent to group studies. Hence, our decision to focus on a singular case. Additionally, this approach allows for the exploration of details of a specific case that large-scale studies may overlook. This depth of insight is especially critical when examining phenomena like BT, where the difference from one practitioner to another could be significant. Using cells instead of humans as targets for treatment eliminates potential placebo effects on the receiver side.

EEG results

When examining whether the participant's physiology differed between the treatment and baseline periods, we observed a global decrease of spectral power in all EEG frequency bands during treatment. Spectral power frequency domains have known associated functions that are consistent with voluntary engagement during treatment periods. Decreases in theta (4–8 Hz) and alpha oscillations are often correlated with attention, emotional regulation, and meditation[27]. Similarly, alpha (8–12 Hz) oscillations are highly involved in inhibitory mechanisms and higher cognitive functions, such as attention, perception, and mental representations of objects and events[28]. An observed decrease in theta and alpha oscillations seems logical, given that engaging in BT treatment requires concentration and focus. These activities are mostly localized in occipital regions, indicating increased visual processing during BT treatment, perhaps consistent with the visualizations of the BT technique that includes "cycling" through images. Beta (18–22 Hz) oscillations are most commonly observed in relation to sensorimotor behavior by decreasing during the preparation and execution of voluntary movements and bursting after the termination of the act[29]. The brain responds similarly when one observes or imagines the movement, even when there is no muscular activity[30]. The participant's intention to treat the cell could be interpreted as a preparatory movement that suppresses beta band activity. Gamma (30–45 Hz or higher) oscillations are associated with the construction of object representation[31]. Because the power in the gamma band increases during complex and attention-demanding tasks, induced gamma activity is often interpreted as the neural substrate of cognitive processes, so a decrease in the gamma band power in the participant could indicate a suppression of higher-level cognitive functions. These decreases in spectral power across various frequency bands during treatment indicate shifts in attention, emotional regulation, meditation, cognitive functions, and sensorimotor behavior that are consistent with the demands of engaging in BT. We also observed a consistent return to baseline immediately after the 15-minute treatment session.

When comparing the treatment of different cell types (live pancreatic cancer cells vs. control target), we observed spectral differences in the beta and gamma frequencies localized over temporal areas. These frequency bands are known to be linked to muscular activity, so any difference in these frequency bands may have no neural origin. Further research is needed to rule out muscular activity as the cause of these findings. However, the Granger analyses showed tubulin cell activity Granger-caused only beta and gamma frequencies, suggesting that the participant's brain is detecting information about the states of the cells.

There was no evidence of significant interaction effects, indicating that the influence of one independent variable (cell type) on the dependent variable (spectral power) did not vary across the different levels of the other independent variable (treatment/baseline). This means the impact of cell type on EEG spectral power remained consistent, irrespective of treatment presence. It suggests that the principal effects of cell type and treatment/control status operate independently.

ECG

The pNN50 HRV measurement showed a slight but significant effect primarily associated with the type of cells involved, indicating decreased activity in the participant's parasympathetic nervous system when treating live pancreatic cancer cells compared to when treating dead cells/medium-no cells. This suggests that the participant might be less relaxed when treating live cells. The RMSSD measure was also lower during the treatment period compared to the baseline period. This decrease in RMSSD points to a reduction in PNS activity for the participant during treatment, suggesting a shift towards greater sympathetic nervous system activation. This may be due to the activation from increased mentation. However, this was not accompanied by a significant increase in heart rate. No interactions were observed. Further studies are necessary to assess if these results are robust and reproducible.

Cell marker results

When comparing whether cell activity, as measured by the three cell markers, differed between treatment versus sham control conditions, we observed significant differences only in the Ca^{2+} measure. Through the 15-minute sessions, Ca^{2+} levels consistently increased for both the BT and sham treatment groups, with the BT group having significantly less of an increase. Ca^{2+} activity is a common marker for cellular response to perturbation and/or communication between cells and is associated with mitochondrial bioenergetic reactions[32,33]. Elevated calcium signaling and intracellular Ca^{2+} levels are associated with cell proliferation, migration, and invasion in various cancer types, including pancreatic cancer[34,35]. Ca^{2+} signaling also plays an important role in cancer cell metastasis by influencing epithelial-mesenchymal transition, cell migration, local invasion, and angiogenesis through cytoskeletal modulation[36]. Therefore, the lower intracellular Ca^{2+} levels observed in the BT-treated PANC-1 cells compared to the sham control supports the anti-invasive effects of BT in PANC-1 cells. This is reinforced in the outcomes from the invasion assay (Fig. 4), as measured 48 h after BT treatment. These findings provide evidence for biological signal changes within the cells due to BT, but do not address the significance of these changes in the overall cancerogenic processes.

Causal influence results

In examining the causal relationship between the participant's physiology data and cell marker data, we observed a significant causal influence of tubulin on EEG and EEG on Ca^{2+} measurements. Tubulin Granger-caused EEG in the beta and gamma frequency bands over the right temporal and occipital channels. EEG in all frequency bands, mostly localized in the left temporal region, Granger-caused Ca^{2+} measurements. β-actin did not Granger-cause any EEG spectral measurements or vice-versa.

One limitation of the Granger analysis is that the 15 min of treatment are considered, including the central 5 min where the participant may move. Movement is likely to induce artifacts in the EEG recording and spectral measurements. Nevertheless, including the central region to compute Granger causality was necessary, as processing 5-minute data chunks both forces the use of model orders below four and dramatically reduces the number of samples to fit for the autoregressive models. Moreover, the robust statistical approach taking into account the sham control cell data allays concerns about the central 5-minute period.

While it is possible to interpret EEG spectral changes during treatment compared to control with respect to the existing literature[15,37], this is not the case for the causal influence of EEG on cell markers and vice-versa. We used surrogate statistics to assess significance. This means we swapped the actual cell marker data during treatment with sham control data collected outside treatment to obtain the null distribution. This type of statistical approach should yield statistically robust results.

The current research project was conducted within the context of preclinical research and only included one cancer cell line. Cell culture studies are the usual first step within cancer treatment discovery research, followed by animal studies. Prior research by our group has documented the effects of BT in multiple cell lines and in animal models, as well as exploring cellular processes[19–22]. However, we acknowledge that as in all cancer treatment research, what is found in cells and animal studies does not always reflect what will happen when scaled up in human clinical studies.

The present study has some limitations as it relates to the equipment used. The fluorescence intensity of tubulin in treatment and sham control cells was measured by two different Cytosmart fluorescent microscopes placed in two different incubators. To reduce any systematic differences due to the microscopes or incubators, the fluorescence intensity of the cells was measured before the treatment at baseline, and the outcome of the tubulin intensity in both BT-treated and sham-treated control cells was calculated by subtracting the baseline, which will minimize any error caused by the differences in the instruments. Another limitation may arise from the sequence and timing of the cells being measured with EVOS M7000. Only one instrument was used to measure intracellular Ca^{2+} and β-actin in both BT-treated and sham-treated control cells, so these markers could not be measured simultaneously in the two groups of cells like was done for tubulin. Again, we measured the baseline of intracellular Ca^{2+} and β-actin in these cells prior to the treatment and normalized the data by subtracting the baseline levels. The Ca^{2+} assay could not distinguish the source for the change in intracellular calcium, increased Ca^{2+} uptake or increased release of bound intracellular Ca^{2+}, and future studies can explore this further. Additional limitations include the BT-treated and control cells having to be plated in two different plates, the cell growth of which could be slightly different. This kind of systemic error might make a more significant difference when the study's outcome was based on the absolute value instead of relative changes as used in the current study. Nevertheless, our positive results warrant follow-up experiments.

Additional limitations in the current study include the specificity of the BT techniques employed and the potential influence of environmental or uncontrolled variables on the participant. As the participant was unaware of the target in terms of cell type or the presence of cells or not, this does not reflect the real-world setting of BT delivery. Yet, it did allow us to conduct the study in a blinded manner. A future study could include

a condition where the participant is told there are cells present or not as a further control. However, the current design was the most blinded we could achieve in this initial model. Yet, we did not control what the participant did, expectations, or thoughts during the sessions and we did not assess physiological outcomes in the sham control participant. The physiological measures were also collected in a continuous manner, and the cell data was every minute, making it more challenging to assess more complex associations. In addition, although the Granger analysis was predictive in both directions, these results do not establish definitive causation per se. However, the application of Granger analysis in this study is contextually appropriate, as it aims to explore potential directional relationships between time series data. The Granger analysis was also conducted post-hoc and undertaken due to the lack of support for entanglement but finding correlations between sets of variables. We also do not know if the changes in EEG spectral power and HRV could reflect general stress/relaxation, concentration, or other nonspecific factors unrelated to BT and changes in participant physiology and cellular outcomes could be due to nonspecific effects. Yet the control for the cellular outcomes does suggest something specific to the participant versus the sham condition. The biological relevance of the changes in Ca^{2+} is unclear, but prior research has linked these changes to increased invasiveness of PANC-1 cells[36–38]. These limitations underscore the need for a cautious interpretation of results and the replication of findings across diverse settings and populations.

The current study did not assess any purported mechanisms of BT. However, our approach removed the risk of placebo effects by focusing on in vitro cellular outcomes rather than patient-reported outcomes like pain or anxiety relief. Subsequent research is needed to replicate and extend our findings in both in vitro and in vivo systems. We expect that quantitative phenomenological models that provide significant predictive power for specific medically relevant outcomes will be developed well before an acceptable mechanistic theory. This course of events is commonplace in medicine and has happened throughout the sciences and throughout history. The current paper offers a basis for further scientific exploration by using rigorous methodologies to address prior criticisms of this field of research.

Conclusion

This study has addressed some limitations in prior non-touch BT research by using a case study design with non-human targets and examining the association between practitioner physiology and cell target types and outcomes. Despite being blinded to the type of cell target being treated, the practitioner's physiology differed between cell target types. Additionally, Granger causality analyses found directional causal associations, both demonstrating the participant's physiology influencing cell activity and cell activity influencing the participant's physiology.

These findings emphasize the complex interactions between physiological responses and the effects on cellular behavior during BT sessions, underscoring the necessity for further research. This endeavor should include rigorous methodological approaches that improve study designs to disentangle the specific components of BT practices contributing to observed outcomes and the conditions under which these effects are most pronounced.

Future investigations could incorporate advanced imaging technologies, standardized protocols for treatment sessions, and more nuanced measures of physiological and cellular responses. Furthermore, interdisciplinary collaborations could provide a more holistic view, combining insights from biophysics, psychology, and complementary medicine to elucidate the underlying mechanisms of action.

Methods

The protocol was pre-registered with Open Science Framework https://osf.io/y8sdn/. The study was approved by the Institutional Review Board of The University of Texas MD Anderson Cancer Center (protocol code 2020 – 1210) and conducted in accordance with the ethical principles outlined in the April 18, 1979 report of The National Commission for the Protection of Human Subjects of Biomedical and Behavioral Research titled "Ethical Principles and Guidelines for the Protection of Human Subjects of Research," also known as "The Belmont Report". The participant provided informed consent before any data collection.

Participant

The unique participant was a male BT practitioner, age 71, using the Bengston Energy Healing Method[38]. Central to this method is the practice of Image Cycling, a process that involves rapidly cycling through a series of mental images of personal desires or outcomes. This practice is designed to enhance the treatment process by engaging the practitioner's focus and energy in a dynamic and fast-paced manner. The technique is mechanical and devoid of any specific belief system. Also, the treatment intent is not a formed or focused concentration on the target, as the practitioner claims he tries to "get out of the way." The participant was one of the most experienced in employing this technique, with over two decades of practice.

Procedure

Data were collected during six 15-minute treatment sessions a day for ten days, for a total of 60 sessions. Each session consisted of five different segments. First, there was a 2-minute control period where the participant rested without cells being present (Pre-Baseline; See Fig. 2). Next, the PANC-1 cells (alive cells or dead cells or medium-no cells) were put in the respective microscopes in a blinded manner, and the participant conducted a 15-minute treatment session: 5 min while seated and remaining still (Treatment 1), 5 min where movements were allowed (Treatment 2), and the last 5 min seated and remaining still (Treatment 3). The cells were then removed, and physiology data were collected for another 2-minute control period (Post-Baseline). The participant was fully blind to the type of cells presented – he was not aware that different cell types were being presented and unaware of the study hypotheses. The experimenter collecting the physiological data was blind to

the cell type but was aware of the study design. The technicians bringing the cell were not blind to the cell type. In 40 sessions, live cells were treated. In 10 sessions, medium- no cells were placed in the microscopes, and in another 10 sessions, dead cells (lysed) were placed in the microscopes. These control sessions were combined, as both conditions lack cellular activity. To have control samples for the cellular outcomes, to control for the potential effects of the equipment, having the presence of a person in front of the cells, and for changes over time on cell outcomes, a sham participant treated 40 matching sets of cells in a different location. The sham participant (not always the same person) adopted the same stance as the BT participant (placement of hand and position). This was done in parallel in real-time with the BT participant's treatment for the tubulin measurement (using two identical CytoSmart Lux FL microscopes) and immediately before the participants' treatment for the Ca^{2+} and immediately after for β-actin (because the same microscope was used). Cell presentation was not done in a random order due to the logistical complexity of cell processing immediately after treatment. Instead, for both participant and sham condition the live cell treatments were done at the same time both before and after the dead cells and the medium-no cells sessions. The order of presentation of dead cells or medium-no cells changed daily. Again, the participant was unaware of the potential groups and assumed all experiments included live cells.

Physiology data collection

Data were collected using an ActiChamp Plus 64 System (BrainProduct Inc.) with a sampling rate of 500 Hz. The 64-channel actiCAP Snap cap was used with electrode names following the 10–20 nomenclature. During cap preparation, electrode impedances were kept below 25 kOhms following the BrainProduct company recommendations. Experimenter AC inserted event markers in the data file during recording for later data segmentation. The ECG attachment to the ActiChamp amplifier was used to collect ECG data. There were 3 ECG electrodes: we placed the negative electrode on the right clavicle, the positive electrode on the left bottom rib, and the ground electrode on the right bottom rib. Electrodermal activity was also collected using the BrainVision GSR Sensor kit. Electro-dermal activity is not analyzed in this report, but it may be included in a subsequent report.

EEG data preprocessing

Experimenters AC and AD imported the EEG BrainVision files and segmented the different data epochs (5 segments times 60 files gave 300 data segments, with the 5 segments corresponding to the two baselines and the three treatment periods). Segment extraction was performed based on the manual markers. Experimenters AC and AD were blind to the type of cells presented to the participant. The data segments were double-checked for length and position using automated scripts. Then, we high-pass filtered the data at 0.5 Hz using a Butterworth 4th-order filter. For pre-registration, we proposed to use a FIR filter. However, both FIR and Butterworth filters showed comparable results in EEG preprocessing[39] with the Butterworth filter, providing slightly narrower and more precise transition bands. The *clean_rawdata* EEGLAB plugin (v2.7) was used to detect bad channels with correlation thresholds of 0.8 and bad segments of data with thresholds of 20 standard deviations, which are the default values and are standard practice in EEG data analysis to balance data quality and preservation[39]. This plugin uses the Artifact Subspace Reconstruction (ASR) method to detect and correct bad portions of data (see Delorme 2023[39]). We only used ASR's algorithm as a detection method and removed the bad data segments instead of correcting them (the default in EEGLAB for offline processing). We then applied Independent Component Analysis (Picard algorithm, standard approach) and the *ICLabel* EEGLAB plugin (v1.4) to detect bad components. *ICLabel* is a machine-learning algorithm that detects artifactual ICA components based on their topography and activity. Each component is assigned a probability of belonging to 1 of 7 classes, which include the muscle and eye movement artifact classes. We applied the *ICLabel* default method to detect eye and muscle artifacts with probability thresholds of 0.9 (on average, one or two components were rejected for each dataset). This type of pipeline is optimal for maximizing significance in EEG experiments[39].

Spectral processing was performed using EEGLAB *std_spec* function using default FFT mode (*specmode* option set to *fft*, and *logtrials* option set to *off*). One-second contiguous and non-overlapping windows are extracted and tapered by a hamming window before computing the FFT. We considered four frequency bands: theta (4 to 8 Hz), alpha (8 to 12 Hz), beta (8 to 22 Hz), and gamma (30 to 45 Hz). Spectral power is averaged across segments for each frequency, log-transformed, and then averaged again for all frequencies within the selected frequency range. The same procedure was applied to the one-minute EEG data segments preceding the cell measurement recordings.

ECG data preprocessing

We processed the ECG data from the healer using the BrainBeats EEGLAB plugin version 1.4[40]. An algorithm detected the QRS complex and R-peaks resulting from sinus node depolarization (i.e., heartbeats), giving us the RR intervals. The RR interval refers to the time elapsed between two successive heartbeats. The algorithm then detected the abnormal R peaks (i.e., artifacts from abnormal cardiac activity or the equipment) to obtain the normal-to-normal (NN) intervals to avoid statistical errors (i.e., the clean RR intervals). We extracted four heart-rate variability (HRV) measures in the time domain: (1) NN-mean, the average duration between heartbeats; (2) NN-SD referring to the standard deviation (respectively) of the time distance between heartbeats; (3) RMSSD referring to the root mean square of successive NN interval differences; (4) pNN50, referring to the percentage of adjacent NN intervals that differ from each other by more than 50 ms (pNN50). We then used the normalized Lomb-Scargle periodogram technique to extract one measure in the frequency domain, namely high-frequency HRV power (HF-HRV). HF-HRV corresponds to spectral power in the 0.15–0.40 Hz frequency band. Other HRV frequency bands – such as low-frequency HRV – could not be estimated because they require longer recording lengths.

Cell analysis and data processing

Cell biology examination was performed by measuring the cytoskeleton markers, i.e. microtubule (MT) and actin, and intracellular calcium in the PANC-1 cells. The cytoskeleton plays an important role in spatially organizing the cell's contents, physically and biochemically interacting with various organelles outside of the cell environment, and generating coordinated forces that allow the cell to move and change shape[41]. Alteration of MTs and microfilaments (actin), polymer structures that orchestrate cellular movement, cell division, intracellular transport, and signaling, is associated with increased migration and metastasis of cancer cells[42]. Additionally, the cytoskeleton appears crucial in the mitochondria's morphology and function, likely mediated via intracellular calcium[33]. In light of discovering the potential role of BT in suppressing the migration and invasion of pancreatic cancer cells[22] and the likely alteration of the cytoskeleton by BT via epigenetic analysis (data not shown), the markers of MT (tubulin polymerization) and microfilaments (actin), as well as intracellular Ca^{2+}, were measured in this study. Prior studies have suggested that biofield therapies may modulate Ca^{2+} signaling pathways, which are essential for regulating cell proliferation, migration, and apoptosis[24,43,44]. Importantly, we found that measures of tubulin, Ca^{2+}, and β-actin change dynamically over a short period of time (data not shown) so they were appropriate assays to assess across a 15-minute period of time.

Measurement of the tubulin polymerization by ViaFluo in the sham control and treatment group was carried out simultaneously with two different CytoSmart Lux FL microscopes (Axion Biosystem, Inc.) located in two different Eppendorf Galaxy 48R CO_2 bench top Incubator with 5% CO2 and temperature set at 37 C (Eppendorf, Burlington, MA).

The intensity of actin (RFP-actin) and intracellular calcium (fluo-4) was measured with the EVOS M7000 Imaging System (Thermo Fisher). Limited by one EVOS M7000 Imaging System, the intracellular Ca^{2+} for the control cells was measured right before the cells were treated with BT, as intracellular Ca^{2+} for the BT-treated cells was measured at the beginning of the experiment (Fig. 2). Conversely, the images of actin in the sham control cells were recorded soon after (less than 5 min in between) the cells being treated with BT as the actin intensity in the BT-treated cells was measured in the last two sets of experiments (Fig. 2). Treatments were provided for 15 min. Each study had two groups: (1) BT treatment group, where cells were either on the stage of the EVOS M7000 microscope on the counter or on the CytoSmart microscope treated through an incubator, or (2) sham-treatment control, where the cells were treated in the same manner for the same amount of time as in the BT group and a person mimicked the movements and distance from the cells as in the BT group. The lab members were instructed not to communicate with the participant about the group assignment, and the participant was blinded to the group assignment.

Cells

Human pancreatic cancer (PANC-1) cells were purchased from the American Type Culture Collection (Manassas, VA). They were maintained in a humidified atmosphere with 5% carbon dioxide at 37∘ C. Cells were routinely cultured in Dulbecco modified Eagle medium with high glucose (Invitrogen Corp, Grand Island, NY) containing 10% fetal bovine serum (Hyclone Laboratories Inc, Logan, UT) supplemented with 50 IU/mL penicillin, 50 µg/mL streptomycin, and 2mM L-glutamine from GIBCO (Invitrogen). RFP-Actin Panc-1 cells were developed using RFP-Actin (Puro) Lentiviral particles expressing a fusion target of RFP-Actin (GenTarget, San Diego, USA). The Lentiviral particles were transduced to Panc-1 cells in the presence of Polybrene (Sigma, St. Louis, MO) in 6 well cell culture plates as per the manufacturer's protocol. After 72 h, the antibiotic Puromycin was added to the wells, and the cells were allowed to grow.

Tubulin, Ca^{2+}, and β-actin measures

Dynamic changes in the microtubule cytoskeleton of PANC-1 cells (tubulin) were monitored by staining the cells with ViaFluor® Live Cell Microtubule-488 dye (Biotium), a cell-permeant probe for staining the microtubule cytoskeleton in live cells. PANC-1 cells ($\sim 5\times10^3$) were seeded to 12 well plates the day prior to the treatment day. Before the treatment, a 2X solution of ViaFluo-488 was made by diluting 2 µL dye with 1mL medium, followed by the addition of 1 µL of verapamil to obtain a working solution. The cells were washed with Calcium/Magnesium-free Dulbecco's PBS, then replaced with ViaFluo-488 working solution and incubated at 37∘ C for 30 min. The staining solution was replaced with fresh medium Fluorobrite DMEM for imaging during the treatment. Fluorescence images of PANC-1 cells were taken every minute during the treatment by CytoSmart Lux FL (Axion Biosystems) with excitation/emission at 452/512 nm. The fluorescence intensity per cell was analyzed using FiJi (ImageJ). Dynamic changes of actin protein were monitored in the RFP-Actin Panc-1 cells during treatment. Stably expressing RFP-Actin PANC-1 cells ($\sim 5\cdot10^4$) were plated in 12-well cell culture plates and allowed to attach overnight prior to treatment. The red fluorescence images were captured every minute in PANC-1 RFP-Actin cells using the EVOS M7000 Imaging System (Thermo Fisher) with excitation/emission at 585/628 nm. Fluorescence intensity was quantified by Celleste Imaging Analysis Software (6.0, Invitrogen).

Fluo-4-AM cell-permeable dye (Invitrogen) was used to measure calcium (Ca^{2+}) mobilization following the manufacturer's instructions. Cells were also plated in 12 well plates as in the cell microtubule cytoskeleton staining assay the day prior to treatment. On the treatment day, cells were washed with PBS and then incubated in Fluorobrite DMEM containing 5 µM Fluo-4-AM dye, organic anion-transport inhibitors probenecid (2mM), and NucBlue, Live ReadyProbes Reagent (Invitrogen) for 30 min at 37∘ C followed by 15-minute incubation at room temperature. During the treatment, the green fluorescent and DAPI images of the cells were captured every minute by the EVOSTM M7000 Imaging System (Thermo Fisher). Fluorescence intensity was quantified by CellesteTM Imaging Analysis Software (Invitrogen). Fluo-4 dye binds to freely diffusible Ca^{2+}, but does not distinguish the source of the change in intracellular calcium, whether it was due to increased Ca^{2+} uptake or increased release of bound intracellular Ca^{2+}.

Tubulin was measured in 40 sessions. Ca^{2+} and β-actin were measured in 20 sessions each since they were using the same apparatus. A measurement was taken every minute automatically (for the second recording, after the baseline), and a marker was manually inserted in the EEG to indicate the beginning of treatment. Note that even though the cell measurement happened at minutes 0, 1, 2,…, 15 of the EEG recording, this only corresponds to the trigger for the camera mounting on the microscope. The camera auto-focus may add a random delay of 5 to 20 s. This delay was ignored in all analyses. For Ca^{2+} and β-actin, measurements were performed on three spots, although for all analyses, we only used the data from the first spot. We used the measurement from the first spot as there was a delay on the images taken in the second or third spot due to the limitation of the instrument, which also caused missing data for spots two and three.

Invasion assay positive control

As a positive control for the overall experiment, the invasiveness of PANC-1 cells was measured using Cytoselect Cell Invasion Assay kits (CBA111, Cell Biolabs, USA) in a 24-well plate format. 1.0×10^6 cells in 300 µL medium without FBS were plated in basement membrane-coated inserts (6 inserts/group). An aliquot of 500 µL of media containing 10% fetal bovine serum (chemoattractant) was added to the lower well of the invasion plate. The control cells and treated cells were plated in two different plates, and they were treated at the same time as in one of the treatment sessions. The inserts were incubated at 37°C for 48 h in a humidified CO_2 incubator after BT or sham treatment. They were then transferred to corresponding clean wells containing cell detachment solutions supplied by the manufacturer. The inserts were further processed as described in the manufacturer's protocol. The endpoint was monitored 48 h after the 15-minute treatment sessions on two separate days across the 10 days of treatment to compare BT treatment to sham control. The fluorescence intensity was measured with a microplate reader at 480 nm/520 nm (Molecular Devices, San Jose, CA).

Statistical analysis

The study utilized a 2 × 2 factorial design, examining a comparison between treatment vs. baseline and cell type, and the interaction between these two factors. EEG spectral and ECG measure statistical analysis was performed using EEGLAB *std_stat* function. The permutation method was used to compute significance, and the false discovery rate method (FDR) to correct for multiple comparisons.

Cell data analysis was performed using the MATLAB *fitglme* function. The independent variables were treatment (treatment vs. no treatment) and minutes (the number of minutes since the treatment had started). We fit the data with the model "cell_measure ~ treatment + (minutes | treatment)," which calculates the significance of the treatment categorical variable knowing the minute continuous variable. We found that for this model, residuals were not normally distributed (Lilliefors goodness-of-fit test of composite normality), so we used surrogate statistics to compute significance where we randomly swapped the data between the treatment and control periods to build the null distribution. We used the model's log-likelihood for the surrogate measure and repeated the procedure 1000 times, shuffling the data at each repetition. We then used the percentile method to calculate the two-tailed significance value. For an estimate of the effect size, we provide the parametric estimate of the estimate divided by the square root of the dispersion of the parametric model (Cohen's d equivalent).

For causality analysis, we first searched for the optimal model order for the autoregressive model. We provided the model with all the 15-minute treatment intervals, all concatenated one after the other, ensuring that at least 8 NaN values separate each 15-minute segment. Adding NaN values between segments forces the autoregressive model to consider the 15-minute segments independently, still fitting them all at once. We used the Akaike Information Criterion[45], which balances model complexity with prediction accuracy, to determine the best model. For each frequency, each channel, and each cell measure, the optimal model order was chosen – according to the Akaike Information Criterion. The reason we stopped at 8 is that at 9, the function we used to estimate the model order (MATLAB *varm* function) became numerically unstable and returned NaN. We obtained the following statistic: order 4 was chosen 252 times, 6 was chosen 762 times, 7 was chosen 327 times, and 8 was chosen 191 times. We thus chose to use a uniform model order value of 6 for all channels and frequencies since it was the most frequent model order.

We then computed Granger causality between each channel in each frequency band and each of the 3 cell measurements (and vice-versa) using the MATLAB *gctest* function. Significance was assessed using surrogate statistics, where we built the null distribution by replacing cell data during treatment with control data collected without the presence of the participant. For every 20,000 iterations (or up to 200,000 iterations for the lowest p-values), we randomly permutated the 15-minute periods of control cell data (note that the data within every 15 min was not permutated). We built the null distribution using the *gctest* function test statistics output. We compared it with the same value for the original periods containing the cell data measurement during treatment by the participant. We computed significance using the percentile methods and corrected for multiple comparisons across all values using the FDR method. We used the NSG service to perform these calculations on the Expanse supercomputer[46].

Data availability

The data was converted to the BIDS EEG format[24] using the EEG-BIDS plugin of the EEGLAB software[43]. It is available on OpenNeuro[47].

Received: 19 April 2024; Accepted: 11 November 2024
Published online: 02 December 2024

References

1. Mao, J. J. et al. Integrative oncology: addressing the global challenges of cancer prevention and treatment. *CA Cancer J. Clin.* **72**, 144–164 (2022).
2. Categories of CAM Therapies | About CAM | Health Information | OCCAM. https://cam.cancer.gov/health_information/categories_of_cam_therapies.htm
3. Ebneter, M., Binder, M. & Saller, R. Fernheilung und klinische Forschung. *Forsch. Komplementärmedizin Klass NaturheilkundeResearch Complement. Cl. Nat. Med.* **8**, 274–287 (2001).
4. Baime, M. J. Review: 'Distant healing' is often effective for improving patient outcomes. *Evid. Based Med.* **5**, 181–181 (2000).
5. Güthlin, C., Anton, A., Kruse, J. & Walach, H. Subjective concepts of chronically ill patients using distant healing. *Qual. Health Res.* **22**, 320–331 (2012).
6. Jain, S. et al. Clinical studies of Biofield therapies: Summary, methodological challenges, and recommendations. *Glob. Adv. Health Med.* **4**, 58–66 (2015).
7. Rao, A., Hickman, L. D., Sibbritt, D., Newton, P. J. & Phillips, J. L. Is energy healing an effective non-pharmacological therapy for improving symptom management of chronic illnesses? A systematic review. *Complement. Ther. Clin. Pract.* **25**, 26–41 (2016).
8. Ernst, E. Distant healing–an update of a systematic review. *Wien Klin. Wochenschr* **115**, (2003).
9. Astin, J. A., Harkness, E. & Ernst, E. The efficacy of distant Healing a systematic review of randomized trials. *Ann. Intern. Med.* **132**, 903–910 (2000).
10. Targ, E. Evaluating distant healing: a research review. *Altern. Ther. Health Med.* **3**, 74–78 (1997).
11. Abbot, N. C. Healing as a therapy for human disease: a systematic review. *J. Altern. Complement. Med.* **6**, 159–169 (2000).
12. Roe, C. A., Sonnex, C. & Roxburgh, E. C. Two meta-analyses of noncontact healing studies. *EXPLORE J. Sci. Heal* **11**, 11–23 (2015).
13. Jain, S. et al. Healing touch with guided imagery for PTSD in returning active duty military: a randomized controlled trial. *Milit. Med.* **177**, 1015–1021 (2012).
14. Lutgendorf, S. K. et al. Preservation of immune function in cervical cancer patients during chemoradiation using a novel integrative approach. *Brain Behav. Immun.* **24**, 1231–1240 (2010).
15. Baldwin, A. L. & Hammerschlag, R. Biofield-based therapies: a systematic review of physiological effects on practitioners during healing. *Explore NY* **10**, 150–161 (2014).
16. Gronowicz, G., Bengston, W. & Yount, G. Challenges for Preclinical investigations of Human Biofield modalities. *Glob. Adv. Health Med.* **4**, 52–57 (2015).
17. Jhaveri, A., Walsh, S. J., Wang, Y., McCarthy, M. & Gronowicz, G. Therapeutic touch affects DNA synthesis and mineralization of human osteoblasts in culture. *J. Orthop. Res.* **26**, 1541–1546 (2008).
18. Gronowicz, G., Secor, E. R., Flynn, J. R., Jellison, E. R. & Kuhn, L. T. Therapeutic touch has significant effects on mouse breast cancer metastasis and immune responses but not primary tumor size. *Evid. Based Complement. Alternat. Med.* **2015**, (2015).
19. Yang, P. et al. Human biofield therapy and the growth of mouse lung carcinoma. *Integr. Cancer Ther.* **18**, 1534735419840797 (2019).
20. Yang, P. et al. Human biofield therapy modulates tumor microenvironment and cancer stemness in mouse lung carcinoma. *Integr. Cancer Ther.* **19**, 1534735420940398 (2020).
21. Yang, P. et al. Biofield therapy suppressed the growth of human pancreatic cancer cells by modulation of cell cycle and cell voltage potentials. *Cancer Res.* **82**, 5382–5382 (2022).
22. Yang, P. et al. Biofield therapy suppressed invasion and metastases of human pancreatic cancer. *Cancer Res.* **84**, 4128–4128 (2024).
23. Kuhn, R. L. A Landscape of consciousness: toward a taxonomy of explanations and implications. *Prog. Biophys. Mol. Biol.* https://doi.org/10.1016/j.pbiomolbio.2023.12.003 (2024).
24. Matos, L. C., Machado, J. P., Monteiro, F. J., Greten, H. J. & Perspectives Measurability and effects of Non-contact Biofield-based practices: a narrative review of quantitative research. *Int. J. Environ. Res. Public. Health.* **18**, 6397 (2021).
25. Fields, C. et al. Search for entanglement between spatially separated Living systems: Experiment design, results, and lessons learned. *Biophysica* **4**, 168–181 (2024).
26. Granger, C. W. Investigating causal relations by econometric models and cross-spectral methods. *Econom. J. Econom. Soc.* 424–438 (1969).
27. Brandmeyer, T. & Delorme, A. Reduced mind wandering in experienced meditators and associated EEG correlates. *Exp. Brain Res.* **236**, 2519–2528 (2018).
28. Clayton, M. S., Yeung, N. & Cohen Kadosh, R. The many characters of visual alpha oscillations. *Eur. J. Neurosci.* **48**, 2498–2508 (2018).
29. Nam, C. S., Jeon, Y., Kim, Y. J., Lee, I. & Park, K. Movement imagery-related lateralization of event-related (de) synchronization (ERD/ERS): motor-imagery duration effects. *Clin. Neurophysiol.* **122**, 567–577 (2011).
30. Neuper, C., Scherer, R., Wriessnegger, S. & Pfurtscheller, G. Motor imagery and action observation: modulation of sensorimotor brain rhythms during mental control of a brain–computer interface. *Clin. Neurophysiol.* **120**, 239–247 (2009).
31. Tallon-Baudry, C. & Bertrand, O. Oscillatory gamma activity in humans and its role in object representation. *Trends Cogn. Sci.* **3**, 151–162 (1999).
32. Leybaert, L. & Sanderson, M. J. Intercellular Ca^{2+} waves: mechanisms and function. *Physiol. Rev.* **92**, 1359–1392 (2012).
33. Kuznetsov, A. V. et al. Crosstalk between mitochondria and cytoskeleton in cardiac cells. *Cells* **9**, 222 (2020).
34. Schnipper, J., Dhennin-Duthille, I., Ahidouch, A. & Ouadid-Ahidouch, H. Ion channel signature in healthy pancreas and pancreatic ductal adenocarcinoma. *Front. Pharmacol.* **11**, 568993 (2020).
35. Wang, W. et al. A complex role for calcium signaling in colorectal cancer development and progression. *Mol. Cancer Res.* **17**, 2145–2153 (2019).
36. Iamshanova, O., Fiorio Pla, A. & Prevarskaya, N. Molecular mechanisms of tumour invasion: regulation by calcium signals. *J. Physiol.* **595**, 3063–3075 (2017).
37. Gasser, T. & Molinari, L. The analysis of the EEG. *Stat. Methods Med. Res.* **5**, 67–99 (1996).
38. Bengston, W. F. & Krinsley, D. The effect of the laying on of hands on transplanted breast cancer in mice. *J. Sci. Explor.* **14**, 353–364 (2000).
39. Delorme, A. EEG is better left alone. *Sci. Rep.* **13**, 2372 (2023).
40. Cannard, C., Wahbeh, H. & Delorme, A. BrainBeats: an open-source EEGLAB plugin to jointly analyze EEG and cardiovascular (ECG/PPG) signals. Preprint at https://doi.org/10.1101/2023.06.01.543272 (2023).
41. Fletcher, D. A. & Mullins, R. D. Cell mechanics and the cytoskeleton. *Nature* **463**, 485–492 (2010).
42. Fife, C. M., McCarroll, J. A. & Kavallaris, M. Movers and shakers: cell cytoskeleton in cancer metastasis. *Br. J. Pharmacol.* **171**, 5507–5523 (2014).
43. Kiang, J. G., Marotta, D., Wirkus, M., Wirkus, M. & Jonas, W. B. External Bioenergy increases intracellular free calcium concentration and reduces Cellular Response to heat stress. *J. Investig. Med.* **50**, 38–45 (2002).
44. Ricardo, S., Alvaro, H. P. & Hordep, V. Effects of Biofield Therapy on Calcium Release in Immortalized Mouse Keratinocyte HaCaT cells. *Public. Health Front.* 18–24. https://doi.org/10.5963/PHF0402002 (2015).
45. Akaike, H. A new look at the statistical model identification. *Autom. Control IEEE Trans.* **19**, 716–723 (1974).
46. Martínez-Cancino, R. et al. The open EEGLAB portal interface: high-performance computing with EEGLAB. *NeuroImage* **224**, 116778 (2021).
47. Cohen, L. et al. The effects of directed therapeutic intent on live and damaged cells. *OpenNeuro*. https://doi.org/10.18112/openneuro.ds005079.v1.0.1 (2024).

Acknowledgements
We thank Helané Wahbeh, Sitara Taddeo, and Mona Sobhani for their helpful comments on the manuscript.

Author contributions
Lorenzo Cohen, Conceptualization, Data curation, Formal Analysis, Funding Acquisition, Methodology, Software, Writing – Original Draft Preparation, Review, Editing, and Final Approval. Arnaud Delorme, Conceptualization, Data curation, Formal Analysis, Methodology, Software, Writing – Original Draft Preparation, Review, Editing, and Final Approval. Andrew Cusimano, Data curation, Writing – Review, Editing, and Final Approval. Sharmistha Chakraborty, Data curation, Writing – Review, Editing, and Final Approval. Phuong Nguyen, Data curation, Writing – Review, Editing, and Final Approval. Defeng Deng, Data curation, Writing – Review and Final Approval. Shafaqmuhammad Iqbal, Data curation, Writing – Review and Final Approval. Monica Nelson, Data curation, Writing – Final Approval. Daoyan Wei, Conceptualization, Methodology, Writing – Review, Editing, and Final Approval. Chris Fields, Conceptualization, Methodology, Writing – Review, Editing, and Final Approval. Peiying Yang, Conceptualization, Methodology, Data curation, Writing – Original Draft Preparation, Review, Editing, and Final Approval.

Funding
This research was funded by the Emerald Gate Charitable Trust, grant number RCTS LS2022-00061373-LK.

Declarations

Competing interests
The authors declare no competing interests.

Ethics declarations
The protocol was pre-registered with Open Science Framework https://osf.io/y8sdn/. The study was approved by the Institutional Review Board of The University of Texas MD Anderson Cancer Center (protocol code 2020 – 1210) and conducted in accordance with the ethical principles outlined in the April 18, 1979 report of The National Commission for the Protection of Human Subjects of Biomedical and Behavioral Research titled "Ethical Principles and Guidelines for the Protection of Human Subjects of Research," also known as "The Belmont Report". The participant provided informed consent before any data collection.

Additional information
Supplementary Information The online version contains supplementary material available at https://doi.org/10.1038/s41598-024-79617-3.

Correspondence and requests for materials should be addressed to L.C.